Glycol-Modified Silanes in the Synthesis of Mesoscopically Organized Silica Monoliths with Hierarchical Porosity

Doris Brandhuber,[†] Viktoria Torma,[†] Christina Raab,[†] Herwig Peterlik,[‡] Alexander Kulak,[§] and Nicola Hüsing*[,||]

Institute of Materials Chemistry, Vienna University of Technology, Getreidemarkt 9, A-1060 Vienna, Austria, Institute of Materials Physics, University of Vienna, Boltzmanngasse 5, A-1090 Vienna, Austria, Centre for Organized Matter Chemistry, School of Chemistry, University of Bristol, Cantock's Close, Bristol BS8 1TS, U.K., and Inorganic Chemistry I, University of Ulm, Albert-Einstein-Allee 11, 89069 Ulm, Germany

Received September 6, 2004. Revised Manuscript Received June 5, 2005

Silica monoliths exhibiting a unique hierarchical network structure with a bimodal pore size distribution and high surface areas were prepared from three different glycol-modified silanes by sol−gel processing. Tetrakis(2-hydroxyethyl)-, tetrakis(2-hydroxypropyl)-, and tetrakis(2,3-dihydroxypropyl)orthosilicate were obtained by transesterification reaction from tetraethylorthosilicate and the corresponding alcohols. The present work shows that, for ethylene glycol- and propane-1,2-diol-modified silanes, simply the release of the corresponding diols during sol−gel processing in the presence of block copolymeric surfactants such as Pluronic P123 results in phase separation on different levels. In addition to an extraordinary cellular network structure with interconnected macropores of several hundreds of nanometers in diameter, the material exhibits a well-ordered mesostructure with periodically arranged mesopores of about 6−7 nm in diameter. Interestingly, the application of glycerol-modified silanes at the given synthesis conditions results in the formation of a disordered silica mesostructure. The architectural properties and the morphology of the gel network cannot only be controlled by the choice of the glycol but also by the amount of acid catalyst in the starting composition.

1. Introduction

The deliberate design of pore sizes over length scales from angstroms to micrometers, of pore orientation, and of the macroscopic morphology of a material has seen considerable progress in recent years. Despite these advances, simultaneous control over all architectural features of an inorganic network is still a very challenging task. Maximum control of the porous structure of oxidic materials can be obtained by combining different synthetic strategies such as templating approaches and sol−gel processing. Molecular templating is well known from the synthesis of the highly organized channel structures of zeolites.[1] In addition to single molecules as templates, also supramolecular arrays of molecules such as lyotropic phases of amphiphilic surfactants or block copolymers can be used as structure-directing agents for a deliberate design of pore systems in the mesoscopic regime.[1,2,3] Other approaches utilize latex spheres for periodically arranged macropores,[4,5] microemulsion droplets,[6−8] or other macromolecules such as bacterial threads.[9] The combination of these templating approaches with sol−gel processing allows for a deliberate shaping of the material as thin films or spheres.[10−12] Even monolithic systems of different sizes have been prepared via an approach termed as direct or true liquid-crystal templating (TLCT) applying relatively high surfactant concentrations of typically more than 30 wt % in water.[13] One of the major problems related to the synthesis of monoliths is the incompatibility of many lyotropic surfactant phases with alcohols, which are inherently released upon hydrolysis and condensation of alkoxysilanes. Thus, the synthesis of materials with a high degree of mesoscopic order in combination with macroscopic morphologies such as large monoliths is still very difficult to achieve, and only a limited number of examples is known from the literature.[14−20] Anderson and co-workers demonstrated a successful route to highly porous surfactant-

* To whom correspondence should be addressed. Tel: +49-731-502 2730. Fax.: +49-731-502 2733. E-mail: nicola.huesing@chemie.uni-ulm.de.
[†] Vienna University of Technology.
[‡] University of Vienna.
[§] University of Bristol.
[||] University of Ulm.

(1) *Handbook of Porous Solids*; Schüth, F., Sing, K. S. W., Weitkamp, J., Eds.; Wiley-VCH: Weinheim, 2002.
(2) Beck, J. S.; Vartuli, J. C.; Roth, W. J.; Leonowicz, M. E.; Kresge, C. T.; Schmitt, K. D.; Chu, C. T.-W.; Olson, D. H.; Sheppard, E. W.; McCullen, S. B.; Higgins, J. B.; Schlenker, J. L. *J. Am. Chem. Soc.* **1992**, *114*, 10834.
(3) Zhao, D.; Feng, J.; Huo, Q.; Melosh, N.; Fredrickson, G. H.; Chmelka, B. F.; Stucky, G. D. *Science* **1998**, *279*, 548.
(4) Holland, B. T.; Blanford, C. F.; Stein, A. *Science* **1998**, *281*, 538.
(5) Park, S. H.; Qin, D.; Xia, Y. *Adv. Mater.* **1998**, *10*, 1045.
(6) Schacht, S.; Huo, Q.; Voigt-Martin, I. G.; Stucky, G. D.; Schüth, F. *Science* **1996**, *273*, 768.
(7) Imhof, A.; Pine, D. J. *Nature* **1997**, *389*, 948.
(8) Schmidt-Winkel, P.; Lukens, W. W.; Zhao, D.; Yang, P.; Chmelka, B. F.; Stucky, G. D. *J. Am. Chem. Soc.* **1999**, *121*, 254.
(9) Davis, S. A.; Burkett, S. L.; Mendelson, N. H.; Mann, S. *Nature* **1997**, *385*, 420.
(10) Brinker, C. J.; Scherer, G. W. *Sol−Gel Science*; Academic Press, 1989.
(11) Lu, Y.; Ganguli, R.; Drewien, C. A.; Anderson, M. T.; Brinker, C. J.; Gong, W.; Guo, Y.; Soyez, H.; Dunn, B.; Huang, M. H.; Zink, J. I. *Nature* **1997**, *389*, 364.
(12) Brinker, C. J.; Lu, Y.; Sellinger, A.; Fan, H. *Adv. Mater.* **1999**, *11*, 579.
(13) Attard, G. S.; Glyde, J. C.; Göltner, C. G. *Nature* **1995**, *378*, 366.

10.1021/cm048483j CCC: $30.25
Published on Web 07/16/2005

templated silica aerogel monoliths using sol−gel processing in the presence of hexadecyltrimethylammonium bromide as a structure-directing agent followed by supercritical drying with liquid carbon dioxide.[18] The resulting material showed hexagonally arranged mesopores within spherical particles, which assemble to give the monolith structure. A significant amount of pores, from interparticle packing, which do not show any periodic ordering, contributes to the materials architecture.

The situation gets even more problematic when materials with pore sizes on different length scales are desired, e.g., materials that combine small (micro- and mesopores) and large (macro-)pores. For these materials, multiple benefits arise from each of the pore size regimes, e.g., micro/mesopores for size- or shape-selective applications and macropores for a reduction of diffusion limitations to the active sites.[21] Thus, the advantages of producing hierarchical pore structures within one material are evident. Dual or multiple templating approaches have been used for the production of materials with a bimodal pore size distribution; however, no morphological control is reported.[22−25] Other, more chemical approaches are based on phase separation strategies in combination with sol−gel processing, e.g., the preparation of monolithic materials for chromatography purposes; however, no or only weak regular arrangements of the mesopores are achieved within a rather bulky network structure in the micrometer range.[26−28]

Nakanishi and co-workers published a series of papers in which they reported the use of water-soluble organic polymers such as poly(ethylene oxide) (PEO) to control macroscopic phase separation parallel to the sol−gel transition.[28] Lindén and Nakanishi extended this approach by applying the macroscopic, PEO, polymer-controlled phase separation of silica particles in combination with an ionic or nonionic surfactant as structure-directing agent in the nanometer regime.[29−31] The material they obtained exhibited interconnected porosity on several length scales, for which the macropore diameter is controlled via PEO−nanoparticle interactions, and the mesopore diameter by the presence of the surfactant, e.g., cetyltrimethylammonium bromide or a poly(ethylene oxide)-based polymer. However, pronounced long-range ordering of the mesopores was not achieved.

As mentioned above, one of the main problems in the synthesis of a monolithic silica-based material with a distinct long-range ordering in the mesoscopic regime is the release of alcohols due to hydrolysis and condensation reactions of the corresponding alkoxysilanes. It is well known that the presence of methanol or ethanol is detrimental to many lyotropic phases as the solvent phase becomes more lipophilic and therefore solvatizes better the hydrophobic regions of the surfactant, which reduces hydrophobic−hydrophilic interactions. Hoffmann and co-workers hydrolyzed ethylene glycol esters of orthosilicic acid in the presence of an ionic surfactant such as tetradecyltrimethylammonium bromide and were able to show by means of small-angle neutron scattering (SANS) that the structure of the surfactant aggregates is not destroyed upon mixing and gelation, thus indicating that the diol-modified silane is compatible with lyotropic surfactant species. However, they did not comment on the structure of the corresponding gels after drying.[32,33]

On this basis, we recently described the synthesis of monolithic silica gels exhibiting a hierarchical network structure with a bimodal pore size distribution (macropores in the range between 200 and 800 nm and periodically arranged mesopores of 8 nm in diameter) from an ethylene glycol-modified silane in the presence of the nonionic block copolymer surfactant Pluronic P123.[34] Pronounced long-range ordering of the mesopores was observed in combination with macroscopic phase separation into one silica-surfactant rich phase and one solvent rich (glycol/water) phase.

The motivation of the present work was to extend this approach of the synthesis of monolithic silica with bi- or multimodal pore size distribution by investigating the influence of other glycols besides ethylene glycol such as propane-1,2-diol or glycerol on the gel structures formed. Because of the different properties of the alcohols, e.g., their polarity, hydroxyl group content, and viscosity, a distinct influence on the formation of the architectural features of the gels is expected. In addition, an optimization of the synthesis procedure with respect to catalyst concentration in order to maximize the degree of mesoscopic ordering will be discussed within the scope of this article. To simplify the following text, the term "glycol" is meant in a way that the compound has more than one alcohol group, thus including the glycerol-modified samples. The use of glycol-modified silanes in combination with a nonionic block copolymer surfactant simplifies the procedures presented by Nakanishi and Lindén significantly, since no supplementary phase separation polymer is required to obtain macrophase-

(14) Bagshaw, S. A.; Prouzet, E.; Pinnavaia, T. J. *Science* **1995**, *269*, 1242.
(15) Göltner, C. G.; Henke, S.; Weissenberger, M. C.; Antonietti, M. *Angew. Chem., Int. Ed.* **1998**, *37*, 613.
(16) Melosh, N. A.; Davidson, P.; Chmelka, B. F. *J. Am. Chem. Soc.* **2000**, *122*, 823.
(17) Feng, P.; Bu, X.; Stucky, G. D.; Pine, D. J. *J. Am. Chem. Soc.* **2000**, *122*, 994
(18) Anderson, M. T.; Sawyer, P. S.; Rieker, T. *Microporous Mesoporous Mater.* **1998**, *20*, 53.
(19) El-Safty, S. A.; Hanaoka, T. *Chem. Mater.* **2003**, *15*, 2892.
(20) El-Safty, S. A.; Hanaoka, T. *Chem. Mater.* **2004**, *16*, 384.
(21) Coppens, M.-O.; Sun, J.; Maschmeyer, T. *Catal. Today* **2001**, *69*, 331.
(22) Yang, P.; Deng, T.; Zhao, D. Feng, P.; Pine, D.; Chmelka, B. F.; Whitesides, G. M.; Stucky, G. D. *Science* **1998**, *282*, 2244.
(23) Velev, O. D.; Jede, T. A.; Lobo, R. F.; Lenhoff, A. M. *Chem. Mater.* **1998**, *10*, 3597.
(24) Antonietti, M., Berton, B.; Göltner, C.; Hentze, H. P. *Adv. Mater.* **1998**, *10*, 154.
(25) Holland, B. T.; Abrams, L.; Stein, A. *J. Am. Chem. Soc.* **1999**, *121*, 4308.
(26) Zhao, D.; Yang, P.; Chmelka, B. F.; Stucky, G. D. *Chem. Mater.* **1999**, *11*, 1174.
(27) Ishizuka, N.; Minakuchi, H.; Nakanishi, K.; Soga, N.; Tanaka, N. *J. Chromatogr. A* **1998**, *797*, 133.
(28) Nakanishi, K. *J. Porous Mater.* **1997**, *4*, 67 and references therein.
(29) Smått, J.-H.; Schunk, S.; Lindén, M. *Chem. Mater.* **2003**, *15*, 2354.
(30) Nakanishi, K.; Takahashi, R.; Nagakane, T.; Kitayama, K.; Koheija, N.; Shikata, H.; Soga, N. *J. Sol−Gel Sci. Technol.* **2000**, *17*, 191.
(31) Sato, Y.; Nakanishi, K.; Hirao, K.; Jinnai, H.; Shibayama, M.; Melnichenko, Y. B.; Wignall, G. D. *Colloids Surf., A* **2001**, *187−188*, 117.
(32) Sattler, K.; Gradzielski, M.; Mortensen, K.; Hoffmann, H. *Ber. Bunsen−Ges. Phys. Chem.* **1998**, *102*, 1544.
(33) Sattler, K.; Hoffmann, H. *Prog. Colloid Polym. Sci.* **1834**, *112*, 40.
(34) Hüsing, N.; Raab, C.; Torma, V.; Roig, A.; Peterlik, H. *Chem. Mater.* **2003**, *15*, 2690. Hüsing, N.; Raab, C.; Torma, V. *Mater. Res. Soc. Symp. Proc.* **2003**, *775*, P.1.7.1.

separated structures. Furthermore, this approach allows and facilitates the formation of highly ordered mesophases.

2. Experimental Section

2.1. Materials. As silanes, tetraethylorthosilicate (Fluka) and trimethylchlorosilane were used without further purification. Ethylene glycol (Aldrich), propane-1,2-diol (Aldrich), and glycerol (Acros), all termed glycols throughout this work, as modifying agents were purified by distillation from Na_2SO_4. As the surfactant and phase separation agent Pluronic P123 ($M_{av} = 5800$); (ethylene oxide)EO_{20}(propylene oxide)PO_{70}(ethylene oxide)EO_{20} (BASF) was applied without any purification.

2.2. Sample Preparation. *Synthesis of the Glycol-Modified Silanes (GlyMSs).* Tetraethylorthosilicate and glycols, ethylene glycol (EG), propane-1,2-diol (PG), and glycerol (GL) were reacted in a molar ratio of 1:4 in an argon atmosphere at 413 K. Ethanol, which is produced during the transesterification reaction, was continuously removed by distillation over a Vigreux column. When no more progress in the reaction could be observed, excess of ethanol and tetraethylorthosilicate was removed in vacuo. The resulting GlyMSs had the following SiO_2 contents (wt %) which were determined by thermogravimetric analysis (TGA): ethylene glycol-modified silane, tetrakis(2-hydroxyethyl) orthosilicate (EGMS, 20 wt % SiO_2); propane-1,2-diol-modified silane, tetrakis(2-hydroxypropyl) orthosilicate (PGMS, 16 wt % SiO_2); glycerol-modified silane, tetrakis(2,3-dihydroxypropyl) orthosilicate (GLMS, 16.5 wt % SiO_2). ^{29}Si(H)-HMBC NMR investigations showed one peak at about −83 ppm for all prepared silanes indicative of a single Si species.

Gel Preparation. Wet gels were prepared by adding EGMS, PGMS, or GLMS to a homogeneous mixture of P123 and aqueous HCl in the concentration range of 0−5 M, resulting in a composition (by weight fraction) of SiO_2/P123/HCl = 10−20/30/70. The mixture was homogenized for 1 min using a vortex stirrer. The liquid mixtures were allowed to gel in a closed PP cylinder at 313 K, and the gels were kept at this temperature for 7 days for aging. The theoretical density of the final dry gels corresponds to approximately 0.07−0.1 g cm^{-3}.

Gels are in the following denoted as GlyMSm(SiO_2), with GlyMS describing the type of glycol-modified silane used (EGMS, PGMS, or GLMS) and m(SiO_2) being the weight fraction of SiO_2 in relation to P123/HCl = 30/70, which was kept constant. All compositions in the text are given by weight fractions, if not mentioned otherwise.

Drying of the Wet Gel Bodies. Drying of the wet gel monoliths was performed by silanization of the whole monolith body with a solution of 10 wt % trimethylchlorosilane in petroleum ether for 24 h, leading to an immediate, visible extraction of the surfactant and aqueous pore liquid. After washing with petroleum ether (three times within 24 h) and ethanol (three times within 24 h), the wet gel bodies were dried by heating them to 473 K (heating rate of 1 K/h) at ambient pressure.[35] Dried samples were also calcined at 723 K for 3 h (heating ramp 5 K/min). Drying is a crucial issue in the synthesis of monolithic gels, but this is discussed in detail elsewhere.[35]

2.3. Characterization. Nitrogen adsorption−desorption isotherms were determined at 77 K using an adsorption porosimeter (Micromeritics, ASAP 2010/2020). Samples were outgassed for 6 h in the degas unit of the adsorption apparatus at 473 K under vacuum prior to analysis.

The Brunauer−Emmett−Teller (BET) surface area was evaluated using adsorption data in a relative pressure range (p/p_0) from 0.05 to 0.2 (S^{BET}). The total pore volume was estimated from the amount adsorbed at a relative pressure (p/p_0) of about 0.99 (V^{N_2}). The mesopore size distribution was calculated on the basis of desorption branches using the BJH model, applying the Harkins−Jura multilayer thickness equation (D^{BJH}).[36] The pore wall thickness was calculated by $2d_{100}^{(SAXS)}/\sqrt{3} - D^{BJH}$.

Mercury porosimetry was applied to determine the macropore volume (V^{Hg}) and macropore size distribution (Pascal 140/440 porosimeter), assuming a contact angle of 130° for the pore size (D^{Hg}) calculations.

Small-angle X-ray scattering (SAXS) measurements were performed using a pinhole camera with a rotating anode generator (Ni monochromated Cu−Kα radiation) and an area detector (Bruker AXS, Karlsruhe). The sample to detector distance was varied from 20 to 98 cm from which scattering curves in the q range 0.1−8 nm^{-1} were obtained. All SAXS patterns were first radially averaged to obtain the function $I(q)$, where $q = (4\pi/\lambda)\sin\theta$ is the scattering vector (2θ = diffraction angle; $\lambda = 0.154$ nm) and then corrected for background scattering from the experimental setup. (The SAXS measurements were carried out on dried as well as calcined gel samples.)

The morphology of the monoliths was investigated by scanning electron microscopy (SEM), which was carried out on a JEOL 6330 FEG-SEM fitted with a secondary electron detector at an accelerating voltage of 10 kV. Samples were coated with a 15 nm thick layer of Pt/Pd using an Agar High-Resolution Sputter Coater. The transmission electron microscopy (TEM) investigations were performed on a JEOL 100 CX TEM with a tungsten filament operating at 100 kV in the bright-field mode.

The ^{1}H, ^{29}Si, and ^{13}C NMR spectra of the liquid precursors were recorded on a Bruker DRX Avance 300 spectrometer at 300.13, 59.62, and 75.43 MHz, respectively. To get a better signal for the glycol-modified silane precursors, ^{29}Si(H)-HMBC NMR measurements were carried out.

3. Results

3.1. Gel Synthesis. The different glycol-modified silanes were prepared by a direct transesterification reaction of tetraethylorthosilicate with the corresponding diol such as ethylene glycol, propane-1,2-diol, or polyol, i.e., glycerol. The term glycol is used to describe all alcohols used in this work. No additional solvent or catalyst is required for this reaction, and the final product is characterized by a defined silicon to glycolate molar ratio which was adjusted to 1:4.5 (EGMS), 1:4.7 (PGMS), and 1:3.7 (GLMS) in our experiments. Complete alcohol exchange was proven by ^{1}H and ^{13}C NMR studies, and ^{29}Si NMR investigations showed a single peak at about −83 ppm for all different GlyMSs. However, ^{29}Si NMR results as well as ^{1}H NMR investigations also indicate an oligomeric or polymeric character of the precursors which is due to the fact that polyols allow the formation of bridged silane species in equilibrium with noncovalently bound polyol, e.g.

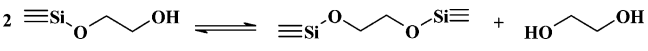

Another possibility might be bonding in a chelating fashion instead of bridging, again resulting in free ethylene glycol

(35) Brandhuber, D.; Hüsing, N.; Torma, V.; Raab, C. K.; Peterlik, H. *J. Mater. Chem.* **2005**, *15*, 1801. Brandhuber, D.; Hüsing, N.; Peterlik, H. *J. Mater. Chem.* **2005**, accepted for publication.

(36) Barret, E. P.; Joyner, L. G.; Halenda, P. P. *J. Am. Chem. Soc.* **1951**, *73*, 373.

Table 1. Synthesis Conditions, Gelation Times, and Physicochemical Properties of Dried Samples Prepared from EGMS[a]

				SAXS	N_2 adsorption−desorption				Hg porosimetry	
Samples	c_{HCl}/M	t_{gel}/min	density/g cm^{-3}	d_{100} (w)/nm	S^{BET}/m^2 g^{-1}	V^{N_2}/cm^3 g^{-1}	D^{BJH} (w)/nm	t_{wall}/nm	V^{Hg}/cm^{-3} g^{-1}	D^{Hg}/μm
EGMS10	0	2	0.16	11.4 (2.9)	1010	1.9	7.8 (1.4)	5.4	5.1	0.45
EGMS10	10^{-3}	3	0.15	11.2 (2.2)	740	2.3	7.0 (2.1)	5.9		
EGMS10	10^{-2}	260	0.18	11.1 (1.0)	960	1.6	6.4 (0.4)	6.4		
EGMS13	10^{-2}	255	0.20	11.1 (1.1)	900	1.2	6.3 (0.8)	6.5		
EGMS17	10^{-2}	250	0.21	11.6 (1.1)	920	1.2	6.7 (0.7)	6.7	2.8	0.75
EGMS20	10^{-2}	245	0.26	12.0 (2.4)	910	1.1	5.7 (1.1)	8.1		
EGMS10	5	120	0.56		830	1.1				
EGMS17	5	10	0.23	11.2 (2.2)	810	1.2	5.6 (2.0)	7.3		

[a] t_{gel} corresponds to the gelation times. The specific surface area, S^{BET}, the total pore volume, V^{N_2}, and pore size distributions with D^{BJH} representing the maximum were determined from N_2 adsorption−desorption experiments. t_{wall} represents the wall thickness of the material and was calculated from the sorption experiments and SAX diffraction data as $[(2d_{100}/\sqrt{3}) - D^{BJH}]$. The value inside the brackets gives the fwhm of the corresponding maximum. V^{Hg} and D^{Hg} represent the macropore volume and the size determined by Hg porosimetry.

Table 2. Synthesis Conditions, Gelation Times, and Physicochemical Properties of Dried Samples Prepared from PGMS

			SAXS	N_2 adsorption−desorption				Hg porosimetry	
Samples	c_{HCl}/M	t_{gel}/min	d_{100} (w)/nm	S^{BET}/m^2 g^{-1}	V^{N_2}/cm^3 g^{-1}	D^{BJH} (w)/nm	t_{wall}/ nm	V^{Hg}/cm^3 g^{-1}	D^{Hg}/μm
PGMS10	0	15	10.8 (5.6)	820	2.7				
PGMS10	10^{-2}	2500	10.1 (1.3)	890	0.8	3.7 (0.6)	5.7	4.3	11
PGMS10	1	250	10.9 (0.9)	960	1.3	5.2 (0.7)	5.5	6.5	5.9
PGMS10	5	150	10.0 (2.2)	860	1.5				

Table 3. Synthesis Conditions, Gelation Times, and Physicochemical Properties of Dried Samples Prepared from GLMS

Samples	c_{HCl}/M	t_{gel}/min	S^{BET}/m^2 g^{-1}	V^{N_2}/cm^3 g^{-1}
GLMS10	0	<1		
GLMS10	10^{-2}	480	800	0.7
GLMS10	1	250	830	0.6
GLMS10	5	20	870	0.5

molecules. In addition, hydrogen-bonding interactions pronounce this polymeric character. These factors lead to unusually long relaxation times in the ^{29}Si NMR spectra and also to more than one signal for the hydroxy protons in the ^{1}H NMR spectra. However, no higher Q species than Q^0 are present in the precursor mixture, proving that the polymeric character is due to intermolecular hydrogen bonding and chelating/bridging glycolate species and not due to (partial) hydrolysis and condensation of the silane.

From these GlyMSs, monolithic silica gels were prepared by addition of EGMS, PGMS, or GLMS to an aqueous liquid crystal (LC) phase of 30 wt % P123 surfactant and in some cases hydrochloric acid in different concentrations. The concentration of P123 in water was kept constant at a ratio of P123/water = 3/7, while the acid concentration has been varied between 0 and 5 M HCl. Both parameters, the type of glycol and acid concentration, have a strong influence on the gelation time and on the formation of the mesostructure (Tables 1−3).

Figure 1 shows the gelation time (t_{gel}) as a function of pH for the different silane precursors. Gelation times under alkaline conditions were not measured because of immediate precipitation of silica from the mixture. Very short gelation times of only a few minutes can be observed at neutral pH (∼6). The mixture turns white before the point of gelation. Upon an increase in the HCl concentration, the gelation time remains constant until pH ∼3.5. Below this value, the gelation time abruptly increases to values of above 250 min. These gels remain transparent for approximately another 250 min after gelation before macroscopic phase separation takes place and the gels turn white. The minimum in the condensation rate (long t_{gel}) is reached around pH 1.5, while further increase of the HCl concentration leads again to a decrease in the gelation times. In addition to the pH dependence, gelation is highly dependent on the SiO_2/P123 ratio, in particular under highly acidic conditions (pH = 0.7). Below 13/30, gelation times constitute around 120 min and transparent gels are obtained at pH = 0.7. Above this ratio, gelation times are much shorter (around 10 min) and white gels are formed (see also Table 1).

Figure 1 also indicates that the type of glycol has a significant influence on the sol−gel reaction rate (Tables 1−3), in particular at neutral pH and around pH 2. The gelation times (at the same pH) decrease in the following order: t_{gel}(PGMS) ≫ t_{gel}(EGMS) > t_{gel}(GLMS) at neutral conditions and t_{gel}(PGMS) ≫ t_{gel}(GLMS) > t_{gel}(EGMS) around pH 2, respectively. The reaction rate of GLMS at neutral pH was so fast that no homogeneous monolithic material could be obtained.

For all materials discussed in the following, white monolithic gel rods with diameters of 10 mm and lengths of 25 mm were obtained. The density of the dry silica gel monoliths was measured by determination of the volume and the weight of the samples and lies in the range of 0.15−0.26 g cm^{-3}.

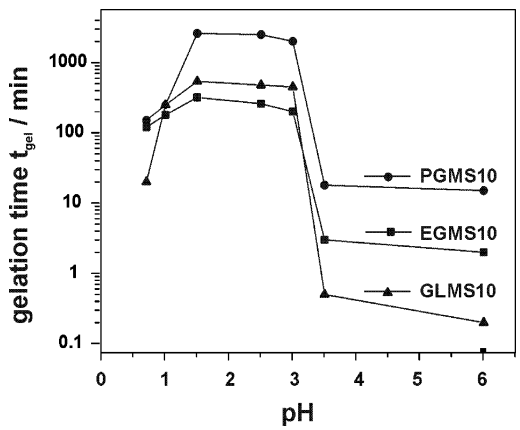

Figure 1. Gelation times as a function of pH of the starting solution for EGMS, PGMS, and GLMS.

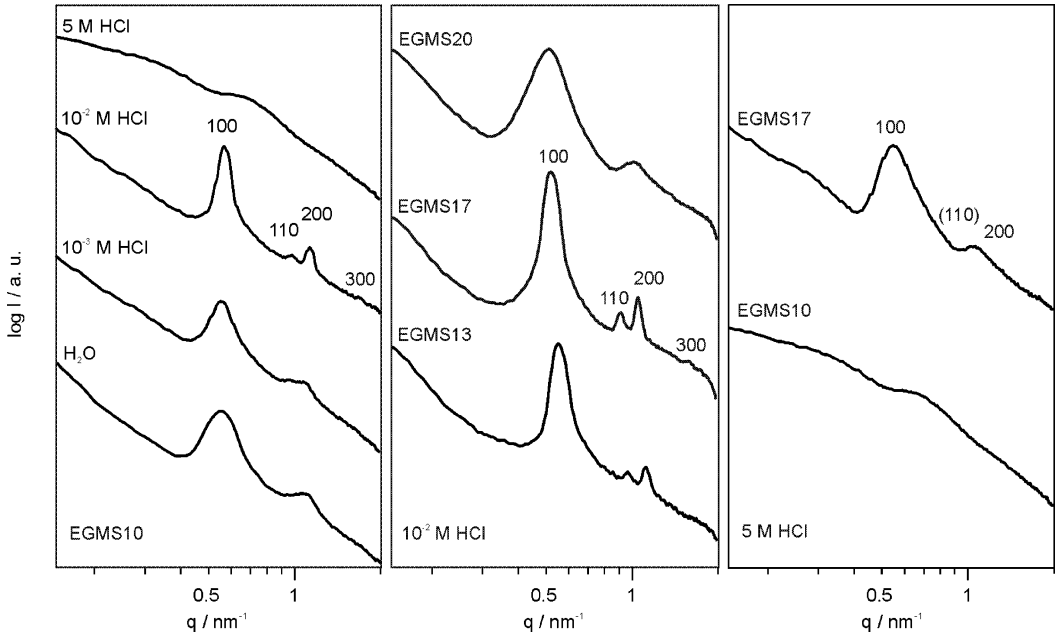

Figure 2. SAXS profiles for dried monoliths prepared from EGMS: (a) for starting composition of EGMS10 at different acid concentrations, (b) at a given acid concentration of 10^{-2} M HCl with increasing amount of EGMS in the precursor sol, and (c) at a given acid concentration of 5 M HCl again with increasing amount of EGMS.

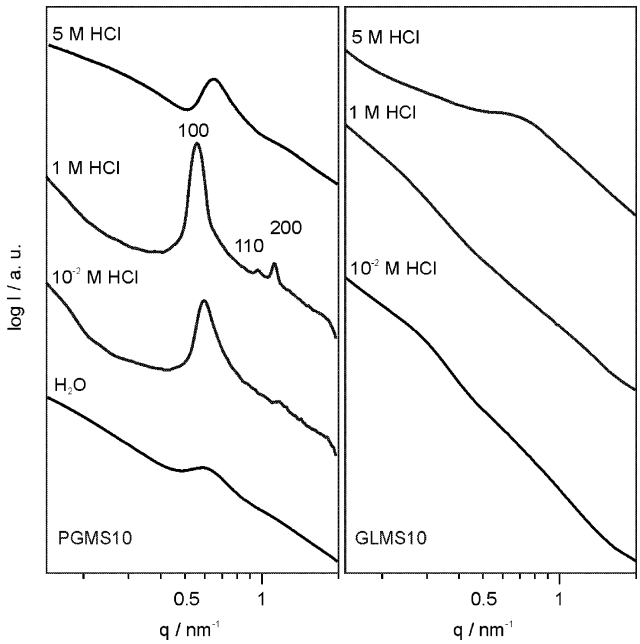

Figure 3. SAXS profiles for dried monoliths prepared from PGMS (left) and GLMS (right) for different acid concentrations.

3.2. Structural Properties of the Resulting Gel Bodies.

SAXS. SAXS patterns were collected for all solids after the drying step and are illustrated in Figures 2 and 3.

In general, samples with an ordered porous structure show up to four distinct Bragg diffraction peaks, which can be indexed to (100), (110), (200), and (300) associated with a *p6mm* hexagonal symmetry with a repeating unit distance of about 11 nm, indicating the formation of highly ordered 2D hexagonal mesostructures. In some samples, the (110) and (200) reflections could not be resolved well due to the broadness of the peaks. The corresponding unit cell parameters of the dried materials from the various GlyMSs can be found in Tables 1−3.

To compare the relative degree of mesoscopic order of the silica materials prepared with different GlyMSs and different acid catalyst concentrations, the values for full width at half maximum (fwhm, *w*) of the (100) diffraction peak have been calculated and are included in Tables 1−3. Some general trends can be observed such that ordered, 2D hexagonal phases could be synthesized with EGMS and PGMS but not with GLMS (Figures 2 and 3).

In addition, the degree of ordering proved to be highly dependent on the HCl concentration used and on the SiO_2/P123 ratio as well. For samples prepared with EGMS and PGMS, resulting in a SiO_2/P123 ratio of 10/30, the degree of mesoscopic order increases with HCl concentration (and gelation time) with maxima at 10^{-2} M HCl for EGMS and at 1 M HCl for PGMS, respectively. At very high HCl concentrations (5 M), this correlation is not valid anymore.

For the EGMS samples (Figure 2), it can clearly be seen that the degree of periodicity within the material depends on the acid concentration as well as on the amount of silane and thus the silane/P123 ratio in the starting mixture. At pH = 0.7, the SiO_2/P123 ratio must be increased to 17/30 to obtain ordered phases at all, and at pH = 2 the optimal ratio for a maximal periodicity was also found at a ratio of 17/30, which corresponds exactly to the SiO_2/P123 ratio for SBA-15 materials. The latter sample prepared with EGMS and 10^{-2} M HCl shows the highest degree of ordering of all materials presented in this publication (Figure 2b − middle curve).

Nitrogen Adsorption−Desorption. Figure 4 shows representative examples taken from the N_2 sorption studies. The N_2 sorption isotherms of the dried materials have been used to obtain information on surface area and mesoporosity. According to the IUPAC classification, type IV isotherms could be observed for all samples.[37] All samples revealing ordered mesostructures in the SAXS studies showed H1 hysteresis loops with more or less sharp adsorption and

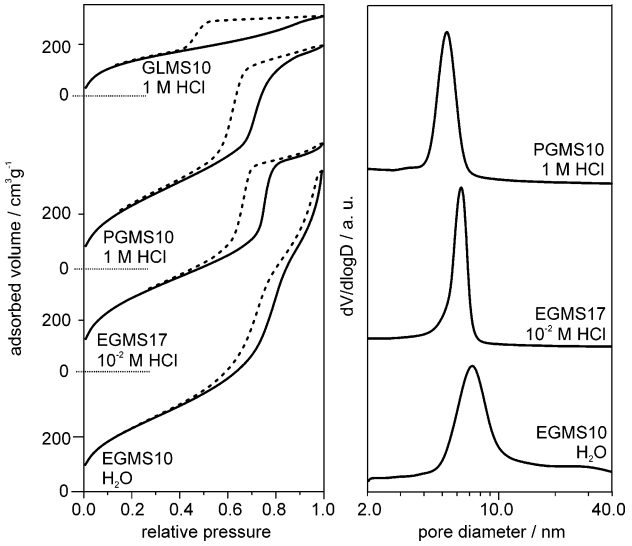

Figure 4. Nitrogen adsorption−desorption isotherm plots and pore size distributions from the desorption branch of hierarchically organized silica monoliths prepared using EGMS, PGMS, and GLMS. The pore size distribution for GLMS samples is not given due to the absence of a uniform pore size.

desorption branches, indicative of the uniformity of pore sizes and shape. The relative sharpness of the desorption branches confirms the same trends as the SAXS studies. The sample prepared under neutral conditions showed the less-defined step in the hysteresis loop in consistence with the SAXS results and revealed the presence of two different types of mesopores. Nonordered samples show H2 hysteresis loops corresponding to more complex pore systems with nonuniform pores. All samples exhibit high specific surface areas S^{BET} between 740 and 1010 $m^2\ g^{-1}$ and high total pore volumes V^{N_2} of 0.5−2.5 $cm^3\ g^{-1}$ (see also Tables 1−3). The total pore volume decreases with an increasing acid concentration in the starting mixture with highest values at neutral conditions and low acid concentrations of 10^{-3} M HCl. It is anticipated that in addition to the mesopores a substantial degree of microporosity attributes to the large surface areas as it is expected for samples templated with lyotropic phases of PEO-containing block copolymers.[38,39] A detailed *t*-plot analysis of samples prepared from EGMS can be found in ref 35.

Pore size distributions (see also Figure 4) of the materials with ordered mesopores have been determined using the BJH model. For comparison, the pore diameter maxima D^{BJH} are listed in Tables 1−3. The BJH method systematically underestimates pore sizes; therefore, only a comparative use of this method is appropriate.[40] In this contribution, we are interested in changes occurring in the pore sizes due to different precursors and synthesis conditions, more than in the absolute value. The values for fwhm (*w*) of the pore size distributions have been calculated in order to compare the relative uniformity of the mesopores of the silica materials prepared with different GlyMSs and catalyst concentrations and are included in Tables 1−3.

The EGMS10 sample prepared with 5 M HCl shows a H2 hysteresis loop and is therefore not considered in the discussion of the pore diameters. For the samples synthesized from EGMS a decrease in the pore diameter with increasing acid concentration is observed starting with 7.8 nm and going down to 5.6 nm. Monoliths prepared from PGMS show the opposite trend (3.7 nm with 10^{-2} and 5.2 nm with 1 M HCl), but the number of samples is not high enough to allow further discussion. GLMS as precursor results only in disordered materials with a H2 hysteresis loop. From the d_{100} spacing and the mean pore size calculated by the BJH method, the wall thickness is calculated and found to be between 5.4 and 8 nm, which is considerably thick compared to other materials templated with nonionic surfactants. As for the pore diameter (D^{BJH}), absolute values cannot be calculated by this method. The wall thicknesses are systematically overestimated, but again, their comparative use is appropriate. For samples EGMS10, the wall thickness increases with acid concentration from 5.4 to 6.4 nm, associated with a decrease in pore size. This trend is reversed for PGMS10 with wall thicknesses of 5.7 nm for 10^{-2} and 5.5 nm for 1 M HCl. Expectedly, higher concentration of silane in the precursor sol increases the wall thickness (up to 8.1 nm, EGMS20). In general, the results from nitrogen adsorption−desorption experiments support the data obtained by SAXS, especially concerning the degree of mesoscopic ordering.

SEM and TEM. Representative electron micrographs of dried gel samples prepared with different silanes are shown in Figures 5 and 6.

TEM images of EGMS17 and PGMS10 (prepared at pH = 2) confirm the well-ordered 2D hexagonal mesostructures with *p6mm* symmetry also found in the SAXS experiments. The estimated repeating unit distance found in the TEM images of about 10 nm corresponds well to the ones obtained from SAXS. SEM studies reveal that parameters such as acid concentration and type of GlyMS not only determine the formation of the mesostructure but also the macrophase/domain separation of the silica/surfactant phase from the solvent phase.

The SEM images reveal interconnected (open) macroporosity but various morphologies for the different samples. The SEM images corresponding to the TEM images shown in Figure 5 can be found in parts b and d of Figure 6. A cellular network built up from rod-shaped aggregates of 2−3 μm in length, and about 0.5 μm in diameter is seen for the EGMS gel (EGMS17), while the PGMS gel (PGMS10) shows a more or less highly aggregated particulate network architecture with monodisperse particles in the range of a few micrometers. In both EGMS and PGMS gels, influences of the acid concentration on the microstructure can be seen. For EGMS gels, the cellular morphology is visible for gels prepared in neutral conditions (EGMS10) but more pronounced and of larger dimensions for the gel with longer gelation times corresponding to a slightly higher acid concentration (parts a and b of Figure 6). Increasing the acid

(37) Sing, K. S. W.; Everett, D. H.; Haul, R. A. W.; Moscow, L.; Pierotti, R. A.; Rouquerol, J.; Stemieniewska, T. *Pure Appl. Chem.* **1985**, *57*, 603.
(38) Smarsly, B.; Göltner, C.; Antonietti, M.; Ruland, W.; Hoinkis, E. *J. Phys. Chem. B* **2001**, *105*, 831. Göltner, C.; Smarsly, B.; Berton, B.; Antonietti M. *Chem. Mater.* **2001**, *13*, 1617.
(39) Kruk, M.; Jaroniec, M.; Ko, C. H.; Ryoo, R. *Chem. Mater.* **2000**, *12*, 1961.
(40) Lukens, W. W.; Schmidt-Winkel, P.; Zhao, D.; Feng, J.; Stucky, G. D. *Langmuir* **1999**, *15*, 5403.

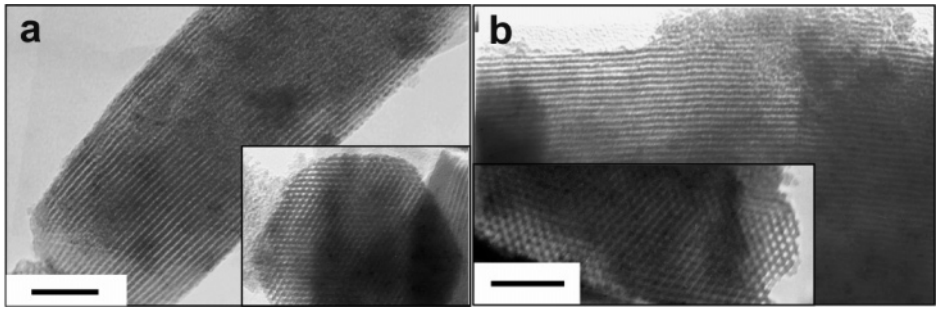

Figure 5. Representative transmission electron micrographs with different orientations of a 2D hexagonal mesostructure with respect to the electron beam. Large pictures, perpendicular to the cylinder axis; small pictures: parallel to the cylinder axis. (a) EGMS17; (b) PGMS10, acid concentration 10^{-2} M HCl, scale bars correspond to 100 nm.

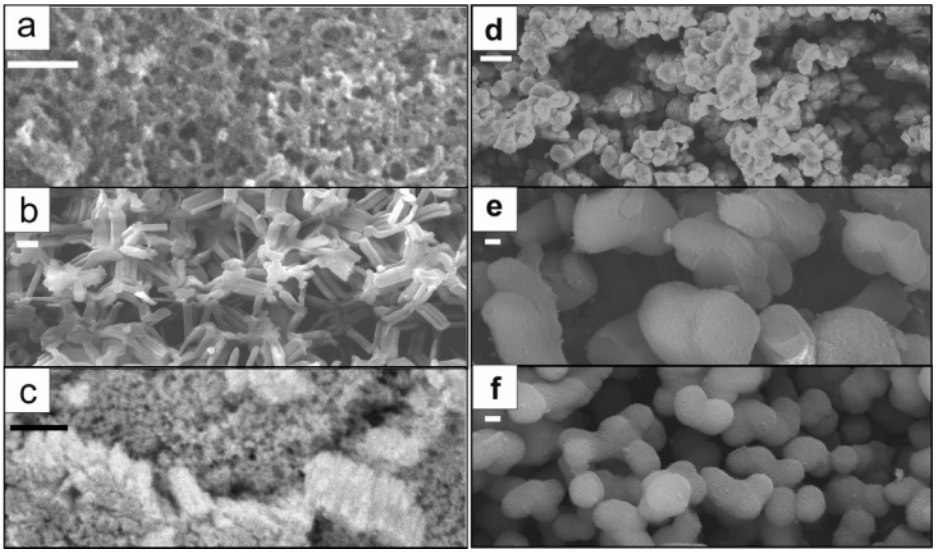

Figure 6. SEM images of samples EGMS10 (a/c), EGMS17 (b), and PGMS10 (d−f) prepared at different HCl concentrations: (a) 0 M, (b/d) 10^{-2} M, (e) 1 M, and (c/f) 5 M. Scale bars: (a/b/c/e/f) 1 μm; (d) 10 μm.

concentration furtheron results in a particulate network structure (Figure 6c) with small particles of around 50 nm; for this sample no periodicity of the mesostructure is observed. Architectural changes can also be found for PGMS gels. Here the structure remains particulate throughout the given set of synthesis parameters but with variations in the size and exact form of the particles. As mentioned, the particle sizes for the gels prepared at pH = 2 are in the range of a few microns with slightly oblated particle morphology. With increasing acid concentration (pH = 1) first a more elongated particle shape evolves, while at pH = 0.7 smaller, monodisperse, spherical particles with diameters of 2 μm are observed (parts d to f of Figure 6). The sample in Figure 6e shows the highest degree in mesoscopic ordering of the PGMS gels (from SAXS data), which is in good agreement with the elongated morphology and larger particle size.

Mercury Porosimetry. Representative intrusion curves and mesopore (from N_2 sorption) and macropore size distributions (from Hg porosimetry) of samples with periodically ordered mesostructures are shown in Figure 7. The experiments revealed the presence of open, uniform macropores with high pore volumes V^{Hg} of $\sim$5 cm^3 g^{-1} for all samples under investigation. The values for macropore volumes and sizes are listed in Tables 1 and 2. Samples with the same silane content of the starting mixture (EGMS10 and PGMS10) have macropore volumes between 4.3 and 6.5 cm^3 g^{-1}. Differences arise from the shrinkage during aging and the drying process, which strongly depends on the stability of the silica network, thus on the pH conditions during network formation. Condensation rates at neutral (H_2O) and highly acidic (1 M HCl) conditions are higher than around moderate acidic conditions (10^{-2} M HCl), which is reflected in the observed macropore volumes. The macroporosity is significantly lower for sample EGMS17 (2.75 cm^3 g^{-1}) due to the higher silane content in the starting mixture. The macropore size distributions are in good agreement with the SEM results and vary significantly for the different silanes and pH conditions between 0.45 and 11 μm. Sample EGMS10 prepared under neutral conditions (H_2O) has the smallest macropore size with 0.45 μm, on the other side of the range lies sample PGMS10 prepared under slightly acidic conditions (10^{-2} M HCl). These findings correlate well with the times of gelation, which can be seen as a measure for the kinetics of phase separation. A high gelation time and therefore late phase separation as observed for sample PGMS10 (10^{-2} M HCl) results in larger domains and as a result also in larger particles and macropores.

After calcination in air at 450 °C for 3 h, the morphology and SAXS patterns of the samples are preserved, confirming that the monolithic material is thermally stable.

4. Discussion

The first part of the discussion addresses the synthesis and hydrolysis/condensation behavior of EGMS, PGMS, and

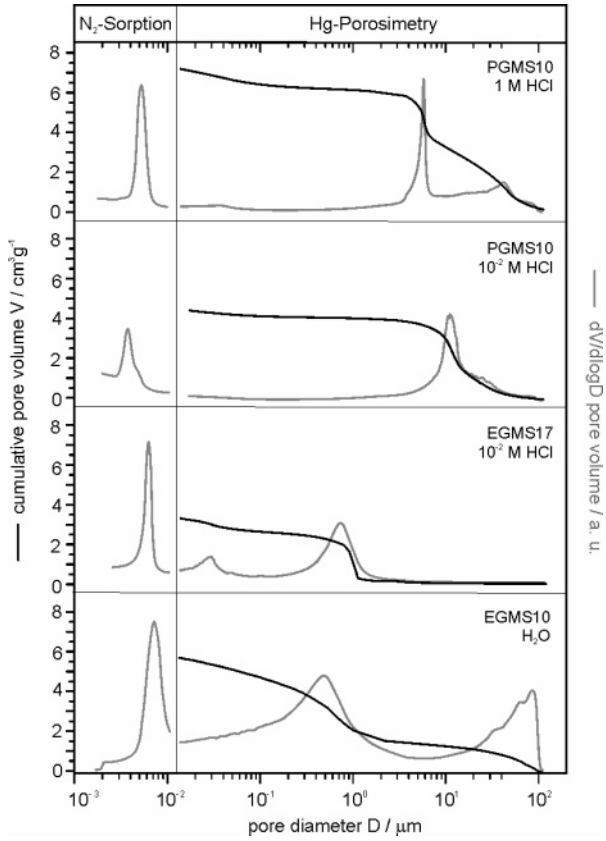

Figure 7. Hg porosimetry intrusion curves and macropore- (Hg porosimetry) and mesopore (N_2 sorption) size distributions showing the bimodal pore structures of representative samples with periodically ordered mesostructures.

GLMS in the presence of Pluronic P123 under different pH conditions, while in the latter part the influence of the different glycols on the resulting materials' structure is discussed.

Sol−Gel Processing with GlyMSs. Modifications of alkoxysilanes with diols or polyols such as ethylene glycol, glycerol, etc., are well known since the middle of the last century; however their application was hampered by their hydrolytic instability.[41,42] Only in recent years has interest in this type of GlyMSs increased again due to some obvious advantages such as (I) a high water solubility (no cosolvent is required to homogenize typical sol−gel solutions), (II) the hydrolysis and condensation reactions can be initiated without acid or base catalysis at neutral pH by addition of water, and (III) hydrolysis results in the release of a biocompatible alcohol. The latter two points were the first ones recognized as a huge advantage in the synthesis of biosilica gels as can be seen in the application of GlyMSs for the encapsulation/immobilization of biomolecules which are otherwise easily denaturated.[43,44]

The extraordinarily high compatibility of EGMS with lyotropic LC phases of surfactant molecules has been demonstrated by Hoffmann in 1997.[32] These silanes are ideal candidates for true LC templating approaches toward the synthesis of nanostructured silica monoliths, especially when nonionic block copolymeric surfactants with polyoxyethylene units as hydrophilic moiety are used as they exhibit analogous chemical properties to the released glycols.

In addition to the work of Hoffmann, Alexandridis and co-workers identified the phase diagrams of aqueous LC phases of similar triblock copolymer surfactants (Pluronic P105) in the presence of different alcohols such as ethanol or glycols, i.e., propylene glycol and glycerol. They demonstrated that, for all investigated systems, regions of lamellar, bicontinuous cubic, hexagonal, and micellar cubic lyotropic phases can be found and that the concentration range of stability of the different phases strongly depends on the polarity of the cosolvent.[45] The ethanolic system showed the largest area of an isotropic solution phase (compared to the area of liquid crystalline phases), which is present at all concentrations above 18 wt % ethanol, while for the glycols LC phases were obtained at much higher concentrations. This corresponds very well to the results obtained in the synthesis of mesostructured silica monoliths, for which it was found that direct LC templating approaches with tetraethoxysilane led to nonordered materials, while removal of ethanol during gel formation resulted in periodically arranged silica structures.

Besides their interesting properties, little is known about the hydrolysis and condensation behavior of GlyMSs. In our studies, the pH was varied from low values (high acid concentration) to the neutral range (using pure water). It can be seen immediately (Figure 1) that the modified silanes show an extraordinary condensation behavior with gel times being very low in neutral conditions, increasing toward pH = 2 and decreasing again in more acidic medium. In sol−gel systems, the typically applied tetraalkoxysilanes such as tetraethylorthosilicate or tetramethylorthosilicate are not miscible with pure water and react very slowly in the neutral regime of the pH scale, considering hydrolysis and condensation reactions.[10] However, GlyMSs are 100% miscible with water; therefore the hydrolysis reactions are very fast. Keeping this in mind, the explanation for the low gelation times at neutral pH and the maximum in the curve in Figure 1 around pH = 2 can be given based on the kinetics known for more common types of tetraalkoxysilanes at different pH. The point of zero charge and isoelectric point of silica and the corresponding siliceous precursors are both around pH 2−4. Above this pH, silica particles carry negative charges and condensation is catalyzed by OH^- ("alkaline" conditions); below pH 2, silica carries positive charges and H^+ acts as the catalyst ("acidic" conditions). The minimum in condensation and therefore network formation rates (gelation time maximum) is normally found around this pH range and corresponds well to the trends observed in the glycol-based systems. The overall reaction rate above this pH range, especially at neutral conditions is governed by the hydrolysis rate which has a minimum at pH = 7 and increases with both the H^+ and OH^- concentration. The extremely high

(41) Goneberg, A.; Verheyden, A. Belgian Patent 510419 (to Union chimique belge Soc.), 1952. Krimm, H.; Schnell, H. German Patent 1136114 (to Farbenfabrik Bayer), 1962. Vaughn, H. A. British Patent 989379, (to General Electric Co.), 1965. Goldberg, E. P.; Powers, E. J. *J. Polym. Sci. Polym. Phys. Ed.* **1964**, *2*, 835.
(42) Mehrotra, R. C.; Narain, R. P. *Indian J. Chem.* **1966**, *5*, 444.
(43) Gill, I.; Ballesteros, A. *J. Am. Chem. Soc.* **1998**, *120*, 8587.
(44) Brook, M. A.; Brennan, J. D.; Chen, Y. WO 03/102001 (to McMaster University, Ontario), 2003.
(45) Ivanova, R.; Lindman, B.; Alexandridis, P. *Langmuir* **2000**, *16*, 3660. Alexandridis, P.; Ivanova, R.; Lindman, B. *Langmuir* **2000**, *16*, 3676.

reaction rates found for the GlyMSs can only be explained by an extremely high hydrolysis rate even under neutral conditions.

The various glycols used in this study show the same trend in the gelation times but different reaction rates, particularly in the more neutral pH range. These observations indicate that the alcohol does have a distinct influence on the reaction kinetics, especially on the hydrolysis rates. The gelation times (at the same pH) decrease in the following order: t_{gel}(PGMS) $\gg$ t_{gel}(EGMS) $>$ t_{gel}(GLMS) at neutral conditions and t_{gel}(PGMS) $\gg$ t_{gel}(GLMS) $>$ t_{gel}(EGMS) around pH = 2, respectively. The reaction rate of GLMS at neutral pH was so fast that no gels but only precipitates were obtained. The reactivity at neutral pH increases with the polarity and relative hydroxyl content of the respective glycol. Around pH 2 the lower SiO_2 content of PGMS (16%) and GLMS (16.5%) compared to EGMS (20%) leads to lower volume fractions of SiO_2 in the overall mixture, when the mass ratio of SiO_2/P123/HCl ratio is held constant, leading to lower gelation times for PGMS and GLMS due to a lower theoretical density (higher solvent content) of the mixture. Another factor in the gelation kinetics might also be the different viscosity (υ) of the respective glycols, which increases in the following order: υ(PGMS) $<$ υ(EGMS) $<$ υ(GLMS). This factor might be another reason for the particularly high gelation time of PGMS around pH = 2. Further studies to investigate the complex sol−gel behavior of these GlyMSs are currently being undertaken by our group.

Structural Properties of the Resulting Gel Bodies. We recently demonstrated that gels prepared from EGMS in neutral conditions show a hierarchical network structure of a cellular silica backbone comprised of macropores in the range of 200−800 nm and periodically arranged mesopores with a repeating unit distance of 11 nm.[34]

At least two competing processes occur simultaneously during network formation; the first process is the sol−gel transition, thus the formation of a solid silica network, and the second is phase separation on different levels, on one hand the formation of supramolecular aggregates of silica/surfactant assemblies which are responsible for the mesoscopic ordering and on the other hand a macroscopic phase separation into condensed silica/surfactant and water/solvent rich domains which define the macroporous structure of the final gel. These processes cannot be viewed independently, since only the relative rates of phase separation and gel formation define the final gel structure. Nakanishi and Takahashi already showed that parameters in the synthesis procedure, which change these relative reaction rates, will have a pronounced influence on the architectural properties of the final gel, including mesoporosity, interconnected macroporosity, degree of macroscopic phase separation and thus the morphology of the material.[28,30,46]

In our previously described system, the reactions were carried out in purely aqueous conditions, with very short gelation times. One of our working hypothesis for this work was that slower condensation rates would give the system more time to evolve and separate the different processes, especially silica condensation from mesoscopic phase separation. We therefore extended the synthesis parameters to acidic media, hoping to increase the degree of long range order in the material, by giving the mesophase more time to evolve. The SAXS profiles of EGMS10 prepared under neutral and under different acidic conditions clearly indicate that the mesoscopic order is more pronounced for systems that have longer gelation times. For the PGMS systems, longer gelation times also favor long-range ordering; however, the structural features are evolved best at pH = 1 instead of pH = 2. This indicates that the processes that govern the structural mesoscopic features of the gel are very complex and highly interconnected, but nevertheless, fine-tuning of the mesostructure is possible by adjusting the experimental parameters.

Solid-phase formation from a liquid phase can be dominated either by a spinodal decomposition or by a nucleation and growth mechanism. The bicontinuous network morphology formed under neutral ("alkaline") conditions, with very short gelation times of only a few minutes, can be explained by a spinodal decomposition mechanism. Under acidic conditions, aggregates built of interconnected particles are formed, which can be understood by a nucleation and (particle) growth mechanism.

The particle morphology itself depends on the silane used; rodlike particles are formed in the case of EGMS and more spherical particles in the case of PGMS. Interestingly, the macrostructure of the EGMS-prepared monoliths resembles to a high degree the structure of rod-type SBA-15 material, which is normally only formed at high ionic strength of the synthesis mixture.[47−49] Even a similar hexagonal shape of the rods can be found for our monoliths prepared at pH = 2, indicating a high degree of mesoscopic order.[50] However, the repeating unit distances are slightly higher in our material (approximately 11 nm) compared to the classical SBA-15 materials prepared from P123 (approximately 10 nm). So far, SBA-15 type of materials prepared via templating with nonionic block copolymers such as Pluronic 123 could only be synthesized under acidic conditions, while in a neutral environment disordered and amorphous silica precipitates.[51] This was attributed to strong electrostatic and hydrogen bonding interactions due to the positive charge the siliceous species carry at pH $<$ 2, thereby promoting cooperative self-assembly. By use of EGMS and PGMS starting materials, these restrictions can be circumvented.

GLMS as a starting material did not result in mesoscopically organized silica under the set of synthesis conditions used in this work. However, getting back to the work of Alexandridis, glycerol also shows a good compatibility with

(46) Takahashi, R.; Sato, S.; Sodesawa, T.; Suzuki, M.; Ogura, K. *Bull. Chem. Soc. Jpn.* **2000**, *73*, 765.
(47) Schmidt-Winkel, P.; Yang, P. D.; Margolese, D. I.; Chmelka, B. F.; Stucky, G. D. *Adv. Mater.* **1999**, *11*, 303.
(48) Boissiere, C.; Larbot, A.; van der Lee, A.; Kooyman, P. J.; Prouzet, E. *Chem. Mater.* **2000**, *12*, 2902.
(49) Yu, C. Z.; Fan, J.; Tian, B. Z.; Zhao, D. Y.; Stucky, G. D. *Adv. Mater.* **2002**, *14*, 1742.
(50) Liu, Z.; Terasaki, O.; Ohsuna, T.; Hiraga, K.; Shin, H. J.; Ryoo, R. *Chem. Phys. Chem.* **2001**, *2*, 229.
(51) Bagshaw, S. A.; Prouzet, E.; Pinnavaia, T. J. *Science* **1995**, *269*, 1242.

lyotropic LC phases; thus it should be possible to obtain mesostructured materials from this precursor as well.

5. Conclusion

Different GlyMSs such as the ethylene glycol, propane-1,2-diol, and glycerol ester of silicic acid have been synthesized and applied in a TLCT approach with the nonionic poly(ethylene oxide)-based block copolymeric surfactant P123 in aqueous (neutral) and acidic conditions. White, monolithic, 3D gels with a hierarchical network structure and an interconnected, multilevel pore system were obtained. The macroscopic gel morphology can be controlled by the choice of glycol to a large extent; PGMS results in gels with a particulate appearance and a very distinct periodicity of the mesophase, while EGMS forms a more cellular network architecture of single rods of 1−3 μm in length and 0.5 μm in diameter with a highly ordered 2D hexagonal mesostructure. Gels prepared from the GLMS did not show any long-range ordering under the given synthetic conditions and exhibit particulate structures typical for silica-based sol−gel materials. For each system, the optimal synthesis parameters such as SiO_2/P123 ratio and acid concentration have to be fine tuned to get optimal results with respect to long-range periodicity of the mesostructure.

The application of GlyMSs in the synthesis of hierarchically structured silica monoliths is facile, rapid, environmentally benign, and does not require the presence of an additional phase separation polymer. This method can readily be extended towards functional monolithic materials for several applications, e.g., chromatographic or separation purposes, support materials or catalysis. Investigations towards monolithic materials exhibiting a different pore structure, chemical functionality, and macroscopic morphology are under way.

Acknowledgment. The authors would like to thank the Wacker Chemie and BASF for their kind donation of chemicals and acknowledge the financial distribution of the Fonds zur Förderung der wissenschaftlichen Forschung (FWF, P16315). V.T. also thanks the FWF for financial support within the scope of a Lise-Meitner Fellowship. We also express our thanks to Dr. M. Puchberger for his assistance with the NMR measurements.

CM048483J